Journal of Applied Electrochemistry **31**: 711–718, 2001.

Role of chromate, molybdate and tungstate anions on the inhibition of aluminium in chloride solutions

S. ZEIN EL ABEDIN*
Electrochemistry and Corrosion Laboratory, National Research Centre, Dokki, Cairo, Egypt
*(*Presently at the Institut für Physikalische Chemie, Lehrstul für Phys. Chemie Kondensierter Materie, Universität Karlsruhe, Kaiserstrasse 12, D-76128 Karlsruhe, Germany)*

Received 17 October 2000; accepted in revised form 5 February 2001

Key words: aluminium, chloride, chromate, inhibition, molybdate, passivation, tungstate

Abstract

The effect of CrO_4^{2-}, MoO_4^{2-} and WO_4^{2-} anions on the inhibition of aluminium corrosion in 0.5 M NaCl solution was investigated. The study comprised potentiodynamic polarization, potentiostatic current–time measurements complemented by SEM–EDAX and XPS investigations. It was found that, the pitting potential of an Al electrode in 0.5 M NaCl solution shifts in the positive direction by addition of CrO_4^{2-}, MoO_4^{2-} and WO_4^{2-} anions, and the shift in potential increases with increase in concentration. A pronounced inhibiting influence was achieved on addition of CrO_4^{2-}, MoO_4^{2-} and WO_4^{2-} anions to the electrolyte during potentiostatic current–time measurements. Chromate anions exhibit a great passivating influence during I/t measurements. This can be explained by the fact that the chromate anion, as a powerful oxidizing agent, is capable of oxidizing the corrosion sites to give a stable Al_2O_3 film. The inhibition observed on addition of molybdate anions is attributed to the adsorption and reaction of MoO_4^{2-} anions on the electrode surface forming a molybdate layer which selectively impedes the ingress of Cl^- ions and hence inhibits the pitting attack. The adsorption of WO_4^{2-} anions at flawed areas and developing pits was found to be the main factor for the observed inhibition.

1. Introduction

Aluminium owes its widespread use and its excellent corrosion resistance to the air formed film that is bonded strongly to its surface. This film is relatively stable in aqueous solutions over a pH range 4–8.5 [1]. In such solutions the surface film is insoluble but may be locally attacked by aggressive anions, primarily chlorides. The effect of Cl^- ions on the pitting corrosion of aluminium and its alloys have been the subject of several studies [2–9]. Many authors [5–9] accept that the mechanism of pit initiation involves: (i) adsorption of chlorides on the oxide surface due to the influence of the electric field at the oxide–solution interface [10]; (ii) formation of a hydroxychloride aluminium salt, which goes into the solution; and (iii) dissolution of the oxide at places where the film is thinner.

Inhibitors that prevent localised attack have been shown to have different effects depending on the stage of the process they inhibit. Hunker and Bohni [11] reported that additives inhibit pit initiation, pit growth, or both. Chromate anions are considered as a good inhibitor for the pitting corrosion of aluminium in chloride solutions, but they have the disadvantage of being poisonous. Therefore, interest has been directed towards the use of other inhibitors with no adverse effects. Based on similarity in chemical structure and expected behaviour between chromate ion and the ions of group VI members of the periodic table, attention was focused on molybdate and tungstate ions. Because of their low toxicity to aquatic species, molybdate and tungstate are being used increasingly as corrosion inhibitors for a variety of metals, including aluminium [12–16]. Several investigators have concentrated on studying the interaction of molybdate with aluminium [17–23]. On the other hand, very little basic work has been devoted to the study of the electrochemical behaviour of aluminium in chloride solutions containing tungstate. Therefore, it seemed of interest to study the effect of chromate, molybdate and tungstate anions on the electrochemical behaviour of aluminium in chloride solutions and to provide additional information on the mechanism of inhibition.

2. Experimental details

Measurements were made on ultrapure aluminium 99.99%. The electrodes were abraded successively with

metallographic emery paper of increasing fineness up to 800 grit, then degreased with acetone and washed with running distilled water. The electrodes were cathodically polarized at –2.0 V vs SCE for 2 min in the test electrolyte, 0.5 M NaCl, before potentiodynamic polarization and potentiostatic current–time measurements. The electrochemical cell was made of Pyrex glass fitted with a platinum auxiliary electrode, separated from the electrolyte by a sintered glass diaphragm, and a saturated calomel reference electrode (SCE). All solutions were prepared from Analar grade reagents and distilled water.

Potentiodynamic polarization measurements were performed using an EG&G potentiostat/galvanostat 273A, controlled by the model 352m corrosion measurement software package. A scan rate of 1 mV s^{-1} was employed and the potential was scanned from –2.0 V up to the breakdown potential. Potentiostatic current–time tests were carried out using a potentiostat–galvanostat (Amel model 2053) with an X–Y recorder (Kipp & Zonen). The treated electrodes were polarized at –740 mV vs SCE in the electrolyte for 20 min. Appropriate amounts of dissolved Na_2CrO_4, Na_2MoO_4 or Na_2WO_4 salts were then added to the electrolyte maintaining the Cl^- ion concentration constant. The solution was agitated slowly by a magnetic stirrer to mix the additives with the electrolyte. A scanning electron microscope (model Philips XL30) attached with energy dispersive X-ray analyser (EDAX) was utilized to examine the electrode surface.

XPS analysis was carried out using a model 550 ESCA/SAM spectrometer (Physical Electronics, USA). The system employed a magnesium X-ray anode ($h\nu = 1253.6$ eV). Binding energies were normalized to that of atmospheric hydrocarbon at 284.6 eV. The vacuum in the analysis chamber was always better than 0.7 μPa. The energy scale was adjusted to match the Au $4f_{7/2}$ peak at 83.8 eV.

3. Results and discussion

3.1. *Polarization measurements*

The effect of adding different concentrations of CrO_4^{2-}, MoO_4^{2-} and WO_4^{2-} anions on the polarization behaviour of Al electrode in 0.5 M NaCl solution was investigated. Figure 1 displays the potentiodynamic polarization curves of Al electrode in 0.5 M NaCl solution without and with different concentrations of CrO_4^{2-} (10^{-4}–10^{-1} M). The polarization curve of Al electrode in 0.5 M NaCl solution is characterized by a flat passive region and the potential at the end of this region, −750 mV vs SCE, represents the breakdown potential at which the onset of pitting attack takes place. The pitting potential of the Al electrode moves in the positive direction on addition of CrO_4^{2-} and the shift in the potential increases with increase in concentration. This signifies the passivating effect of CrO_4^{2-} anions on the pitting attack of Al electrode in chloride solutions.

Addition of MoO_4^{2-} causes a large shift in the pitting potential of Al electrode in the positive direction, Figure 2, indicating the greater inhibiting influence of MoO_4^{2-} anions. The pitting potential shifts in the positive direction with increase in MoO_4^{2-} concentration and the maximum shift is recorded at $C = 10^{-1}$ M MoO_4^{2-}, where the electrode remains passive until a potential value of –240 mV is reached. This can be attributed to the formation of a thick layer of molybdate on the electrode surface, during cathodic polarization, which restricts the adsorption of Cl^- ions at the electrode surface and hence inhibits pitting.

The polarization curves of Al in 0.5 M NaCl solution free from and containing different concentrations of WO_4^{2-} anions are displayed in Figure 3. The pitting potential moves in the positive direction on addition of WO_4^{2-}, signifying the inhibiting effect of tungstate anions. The extent of displacement of the pitting

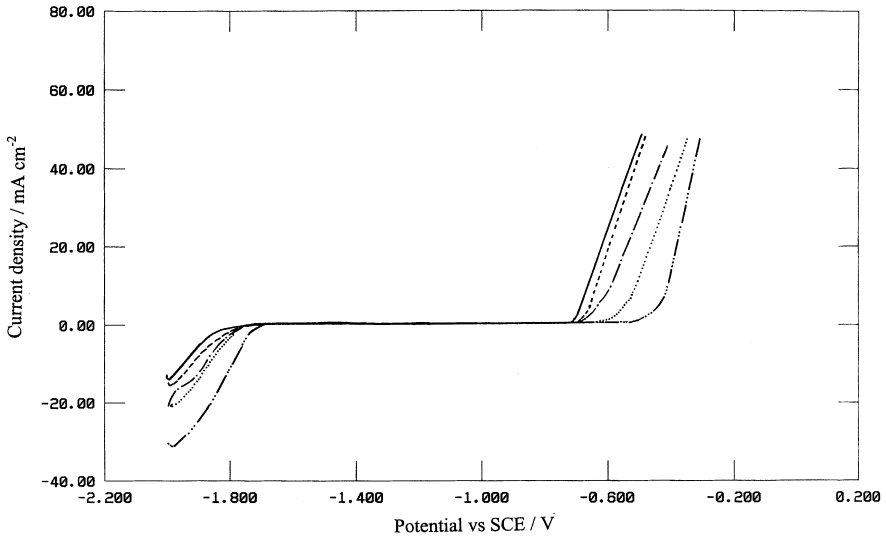

Fig. 1. Potentiodynamic polarization curves of Al electrode in 0.5 M NaCl solution and different concentrations of CrO_4^{2-}. Curves (—) without CrO_4^{2-}, (- - - -) 10^{-4} M CrO_4^{2-}, (– · –) 10^{-3} M CrO_4^{2-}, (···) 10^{-2} M CrO_4^{2-} and (–···–) 10^{-1} M CrO_4^{2-}.

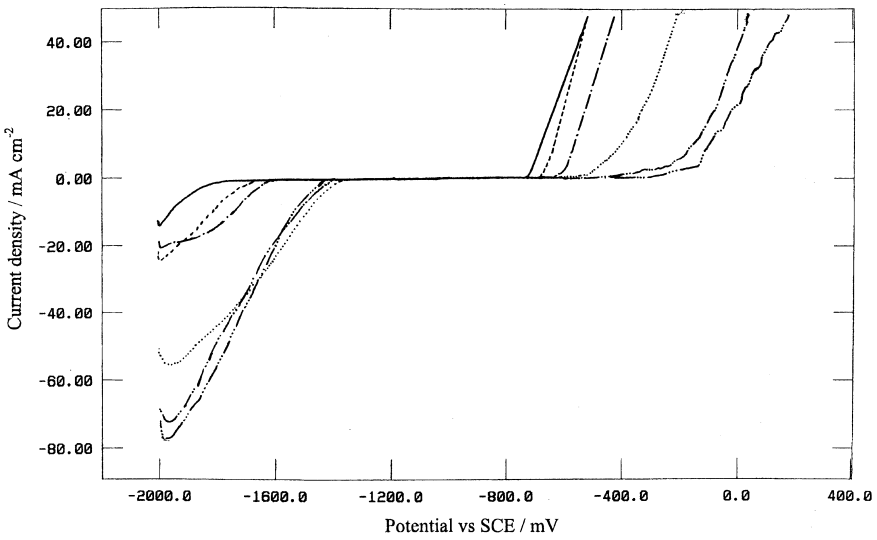

Fig. 2. Potentiodynamic polarization curves of Al electrode in 0.5 M NaCl solution and different concentrations of MoO_4^{2-}. Curves (—) without MoO_4^{2-}, (- - - -) 10^{-4} M MoO_4^{2-}, (– · –) 10^{-3} M MoO_4^{2-}, (· · ·) 10^{-2} M MoO_4^{2-}, (–··–) 5×10^{-2} M MoO_4^{2-} and (–· · ·–) 10^{-1} M MoO_4^{2-}.

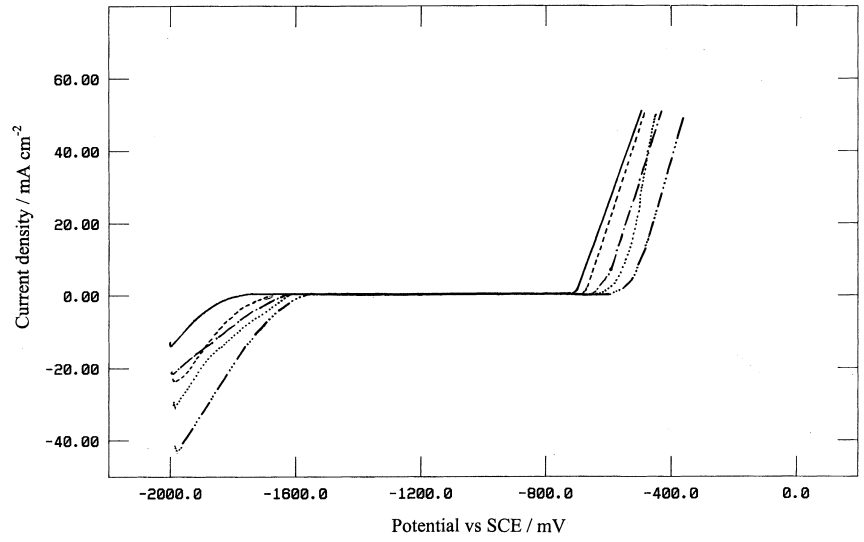

Fig. 3. Potentiodynamic polarization curves of Al electrode in 0.5 M NaCl solution and different concentrations of WO_4^{2-}. Curves (—) without WO_4^{2-}, (- - - -) 10^{-4} M WO_4^{2-}, (– · –) 10^{-3} M WO_4^{2-}, (· · ·) 10^{-2} M WO_4^{2-} and (–· · ·–) 10^{-1} M WO_4^{2-}.

potentials is not as high as that observed with comparable concentrations of MoO_4^{2-} anions.

3.2. *Current–time measurements*

The potentiostatic current–time measurements during metastable activation repassivation were used to evaluate the inhibiting influence of CrO_4^{2-}, MoO_4^{2-} and WO_4^{2-} under highly aggressive test conditions. This can give valuable information about the mechanism of inhibition. The aluminium electrode was polarized for 20 min at –740 mV in 0.5 M NaCl solution. These conditions are sufficient to promote the onset of pitting attack. Appropriate amounts of CrO_4^{2-}, MoO_4^{2-} or WO_4^{2-} were then added to the test electrolyte maintaining the Cl^- ion concentration constant. The applied potentials were still maintained at –740 mV vs SCE. Typical I/t profiles are shown in Figure 4. As shown, before addition of the inhibiting agents, the curves exhibit a rapid decrease in the anodic current in the early moments. Then the current fluctuates with high frequency having an amplitude of approximately 70 μA, indicating the onset of metastable pitting attack. On addition of CrO_4^{2-}, 0.1 M, after 20 min, the anodic current decreases rapidly without fluctuations and takes a constant value (1.7 μA), indicating the immediate inhibition to the pitting attack. This can be explained by the fact that the chromate anions, as a powerful oxidizing agent, are capable of oxidizing the corrosion sites to give a stable passive film of Al_2O_3 which covers the whole electrode surface. The SEM–EDAX examination of the surface after potentiostatic I/t measurements at –740 mV in 0.5 M NaCl and 0.1 M CrO_4^{2-} solution supports the above discussion, Figure 5. As can be seen in the SEM

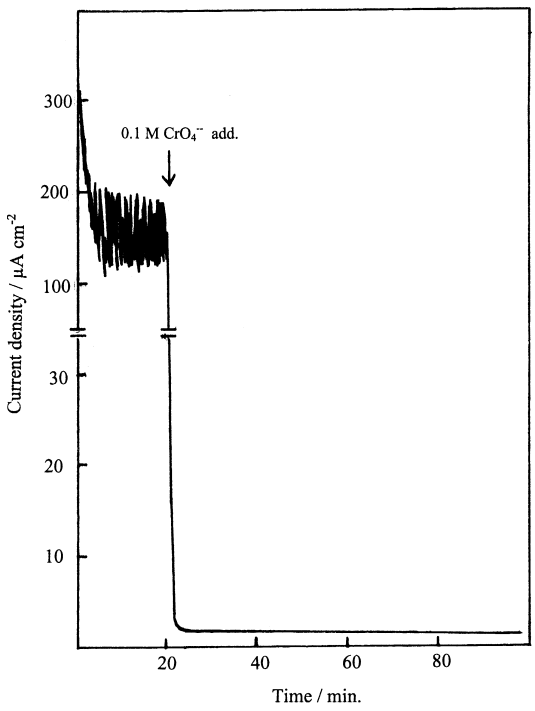

Fig. 4. Potentiostatic current–time plot of Al electrode polarized at −740 mV in 0.5 M NaCl solution to which 0.1 M CrO_4^{2-} was added after 20 min.

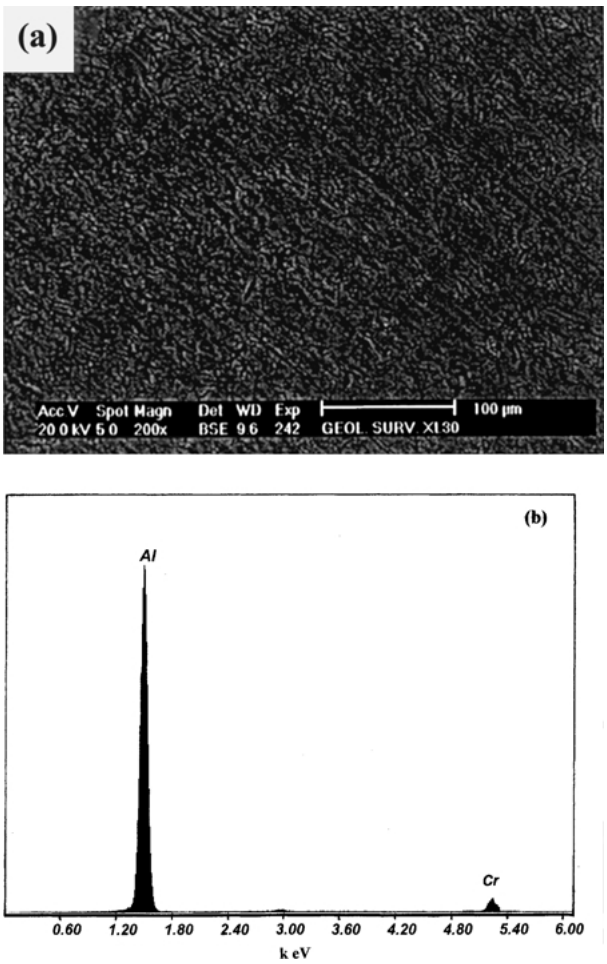

Fig. 5. (a) SEM micrograph of Al electrode obtained after potentiostatic polarization at −740 mV in 0.5 M NaCl + 10^{-1} M CrO_4^{2-}. (b) EDAX analysis of the area shown in the micrograph.

micrograph of Figure 5(a), complete passivation is achieved since there is no attack on the surface. A very low amount of Cr was detected on the surface by the corresponding EDAX profile, Figure 5(b), indicates that the oxidizing power of chromate as a passivator is the main cause in the inhibition process.

Molybdate shows almost the same inhibiting influence as chromate but the value of the anodic current after addition of MoO_4^{2-}, 0.1 M, is higher than that observed in the case of CrO_4^{2-}, Figure 6. Moreover, slight fluctuations in the current were noticed but these were of low frequency and magnitude with an amplitude of about 1 μA. This indicates that the inhibiting effect of MoO_4^{2-} is not as strong as that of CrO_4^{2-}. The SEM–EDAX examination of the surface after potentiostatic I/t measurements at –740 mV in 0.5 M NaCl and 0.1 M MoO_4^{2-} solution is displayed in Figure 7. A mud-crack structure is seen in Figure 7(a) and a high concentration of Mo is detected by the corresponding EDAX analysis, Figure 7(b). This indicates the adsorption and reaction of MoO_4^{2-} anions at the electrode surface and formation of a salt layer, but complete passivation is not achieved.

XPS analysis of the surface layer of the Al electrode after polarization at –740 mV in 0.5 M NaCl solution, to which 0.1 M MoO_4^{2-} solution was added after 20 min, can give additional information about the chemistry of the surface film formed on the electrode. The Mo(3d), Al(2p) and O(1s) spectra are shown in Figure 8. The Mo(3d) spectrum, Figure 8(a), revealed three peaks at 230.1, 232.6 and 234.4 eV, identified as MoO_2, MoO_4^{2-} and MoO_3, respectively [24, 25]. It is clearly seen, from the intensity of the three peaks, that the major constituent present is MoO_4^{2-} species. Therefore, it can be concluded that MoO_4^{2-} anions adsorb onto the surface and form a molybdate layer, which selectively impedes the ingress of Cl^- ions and hence inhibits the pitting attack. It was stated that MoO_4^{2-} restricts the ingress of Cl^- by forming a highly charged film [26]. Also, a molybdate species has been found in the passive film of Al–Mo alloys in chloride solutions and has been shown to govern the pitting process [24, 27]. In both the Al–Mo alloys and Al exposed to molybdates in solution, the breakdown potential is driven to more noble potentials, and becomes resistant to pitting attack. The similarity in the two cases is further evidence that the molybdate in the film serves to selectively restrict the ingress of Cl^-, thereby preventing pitting.

The Al(2p) spectrum of Figure 8(b) shows two peaks at 72.2 and 74.4 eV which belong to Al in the substrate and Al_2O_3, respectively [28]. The peak associated with Al_2O_3 contributes most of the signal, indicating the formation of a relatively thick passive film.

The oxygen peak obtained from the electron spectroscopy chemical analysis, Figure 8(c), has a width of 3.5 eV, indicating that it is caused by a sum of several overlapping peaks and confirming the presence of

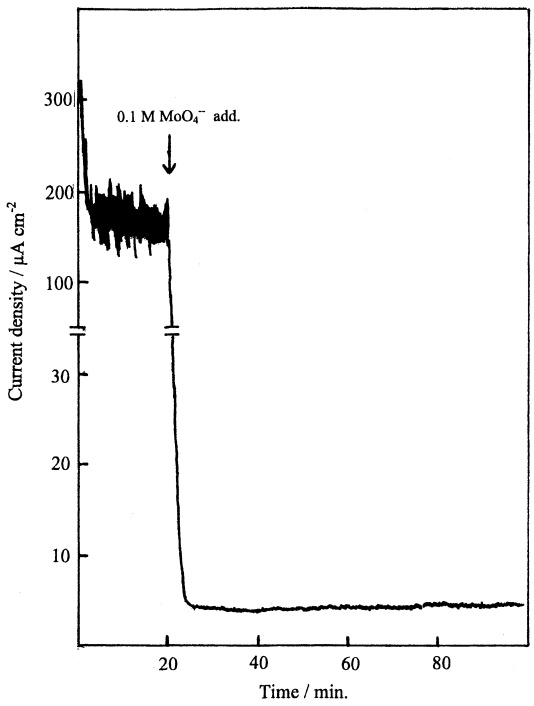

Fig. 6. Potentiostatic current–time plot of Al electrode polarized at −740 mV in 0.5 M NaCl solution to which 0.1 M MoO_4^{2-} was added after 20 min.

oxygen in different forms. This conclusion is supported by the XPS peaks in Figure 8(a) and (b) which indicate that the most probable chemical forms of oxygen are MoO_2, MoO_4^{2-}, Mo_2O_3 and Al_2O_3.

The introduction of WO_4^{2-}, 0.1 M, to the test electrolyte after polarization at –740 mV for 20 min, has a small effect in promoting the onset of passivation of the metastable pits. As shown in Figure 9, on addition of WO_4^{2-}, the anodic current decreases but remains fluctuating with an amplitude of approximately 7 μA. This signifies that complete passivation conditions are never achieved.

The effect of additive concentration on the inhibition of Al during I/t measurements was studied. It was observed that the inhibiting effect of these additives increases with increase in concentrations (from 10^{-4} to 10^{-1} M) and that at the same concentration, the inhibiting effect of the additives increases in the following order:

$$CrO_4^{2-} > MoO_4^{2-} > WO_4^{2-}$$

This can be attributed to the greater oxidizing power of CrO_4^{2-} as a passivator compared to MoO_4^{2-} and WO_4^{2-} anions.

3.3. *Mechanism of inhibition*

It seemed of interest to highlight the role of CrO_4^{2-}, MoO_4^{2-} and WO_4^{2-} in the inhibition process. During the polarization of aluminium electrode at −740 mV in

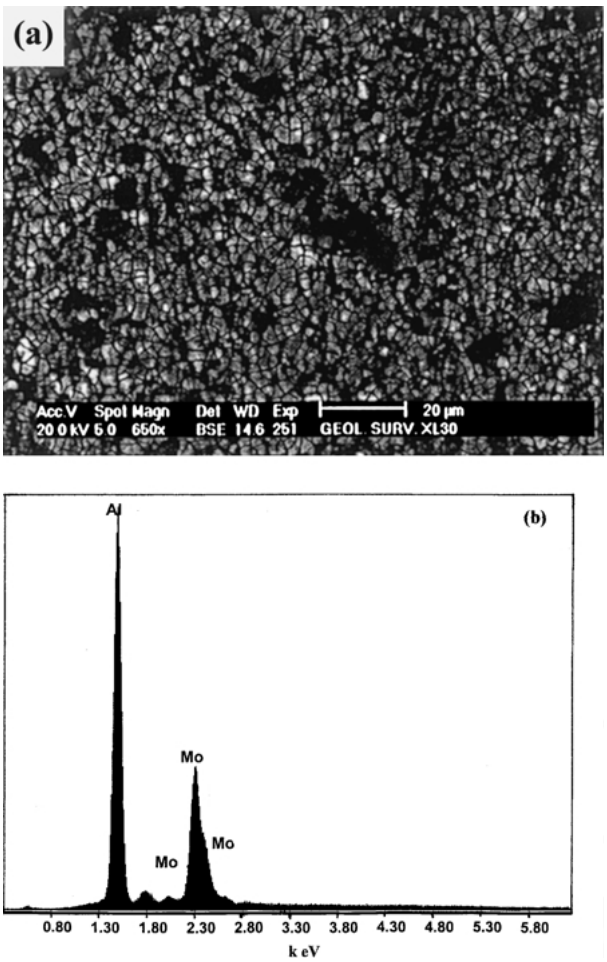

Fig. 7. (a) SEM micrograph of Al electrode obtained after potentiostatic polarization at −740 mV in 0.5 M NaCl + 10^{-1} M MoO_4^{2-}. (b) EDAX analysis of the area shown in the micrograph.

0.5 M NaCl solution, species such as $Al(OH)Cl^+$ and $AlCl^{2+}$ may exist, giving rise to the relatively stable $Al(OH)_2Cl$ complex, reported in pit initiation studies [29, 30]. It has been postulated [29] that the initiation of the pitting of aluminium in chloride solutions proceeds in four consecutive steps: (i) the adsorption of Cl^- on the oxide film; (ii) the chemical reaction of the adsorbed anion with the Al^{3+} in the oxide lattice; (iii) the thinning of the oxide film by dissolution and (iv) the direct attack of the exposed metal by the aggressive anion with the formation of transient complexes which rapidly undergo hydrolysis. Thus,

$$Al^{3+} + 4\,Cl^- \rightarrow AlCl_4^- \quad (1)$$

$$AlCl_4^- + 2\,H_2O \rightarrow Al(OH)_2Cl + 2\,H^+ + 3\,Cl^- \quad (2)$$

The incorporation of these complexes into the oxide film may result in the generation of flaws at which the adsorption of the passivating agent occurs competing with the adsorption of the chloride anions at the same points.

Chromate solutions, in the acidic conditions generated in developing pits, are powerful oxidizing agents and

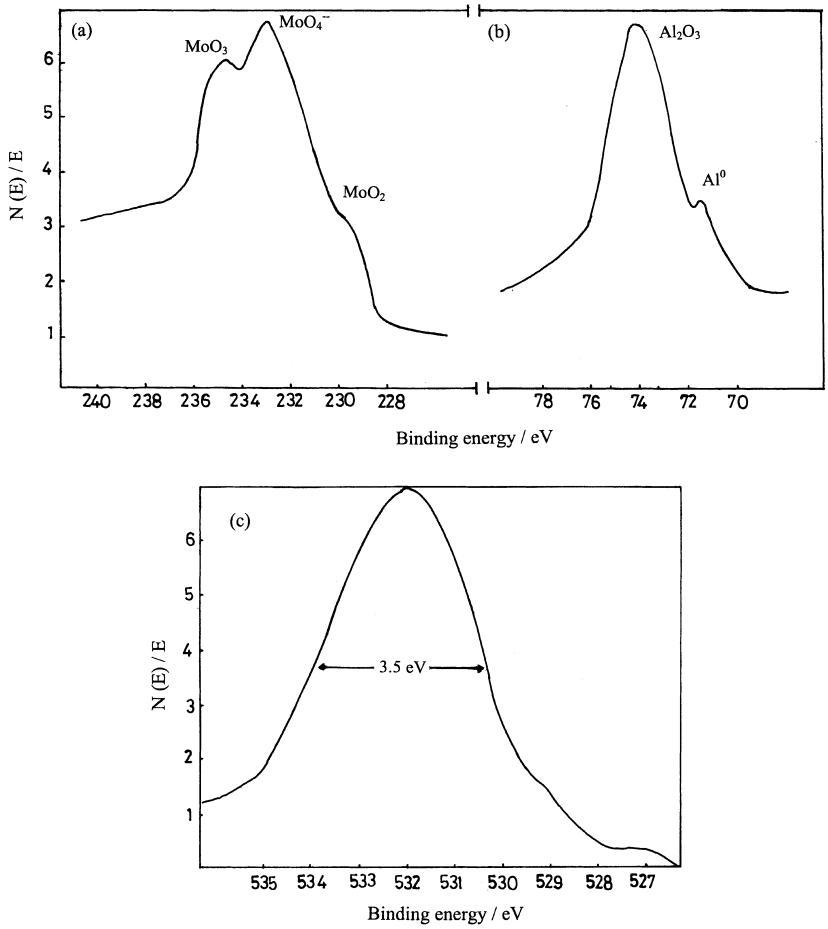

Fig. 8. XPS spectrum of (a) Mo(3d), (b) Al(2p) and (c) O(1s) measured for Al electrode after potentiostatic current–time measurements at −740 mV in 0.5 M NaCl and 10^{-1} M MoO_4^{2-} solution.

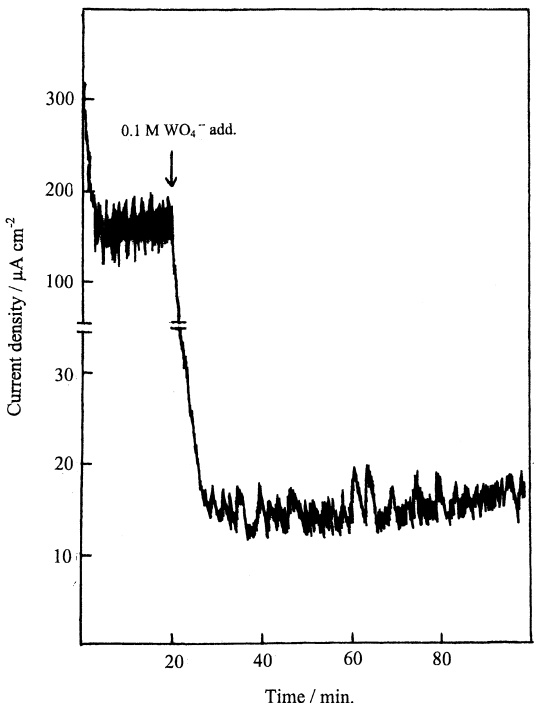

Fig. 9. Potentiostatic current–time plot of Al electrode polarized at −740 mV in 0.5 M NaCl solution to which 0.1 M WO_4^{2-} was added after 20 min.

therefore, the CrO_4^{2-} anion is involved in an oxidation–reduction reaction which leads to the formation of a stable hydrated oxide film as follows:

$$2\,Al + 2\,CrO_4^{2-} + 10\,H^+ \rightarrow Al_2O_3 \cdot 3\,H_2O + 2\,Cr^{3+} + 2\,H_2O \qquad (3)$$

The inhibiting effect of MoO_4^{2-} is due to the adsorption of molybdate at the electrode surface forming a barrier layer which impedes the adsorption of Cl^- ions on the electrode surface. Moreover, the partial oxidizing effect of molybdate enhances the oxidation of the corrosion sites to a stable oxide film according to the redox reaction:

$$2\,Al + 3\,MoO_4^{2-} + 6\,H^+ \rightarrow Al_2O_3 \cdot 3\,H_2O + 3\,MoO_2 \qquad (4)$$

In the case of WO_4^{2-}, the adsorption of WO_4^{2-} anions at flawed areas and developing pits is the main factor for the observed inhibition effect. However, the formation of a complete surface layer of WO_4^{2-} looks to be very difficult, and hence complete passive conditions are never achieved. This can be confirmed by SEM–EDAX examination of the electrode surface after potentiostatic

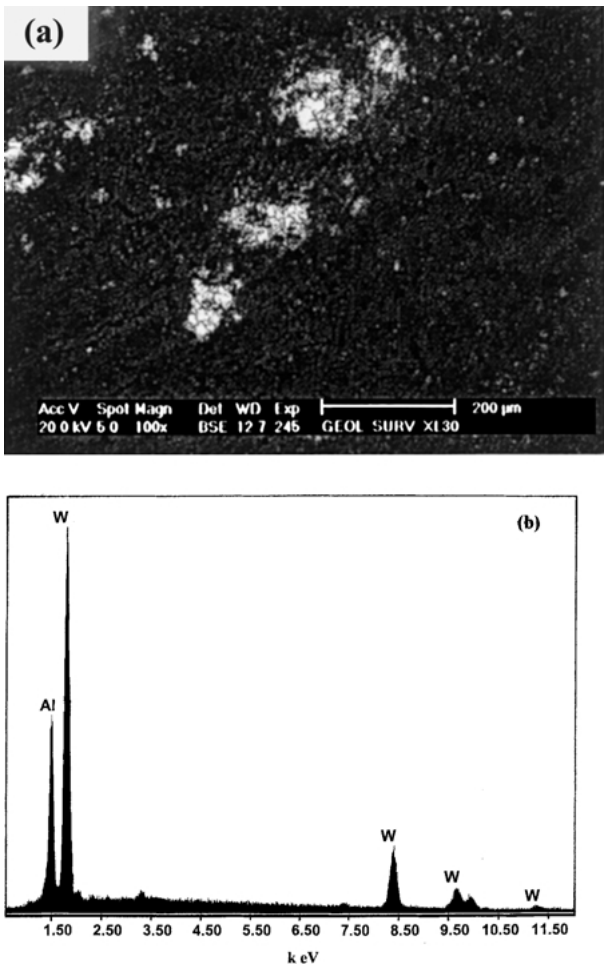

Fig. 10. (a) SEM micrograph of Al electrode obtained after potentiostatic polarization at −740 mV in 0.5 M NaCl + 10^{-1} M WO_4^{2-}. (b) EDAX analysis of the white areas shown in the micrograph.

I/t measurements in 0.5 M NaCl and 0.1 M WO_4^{2-}. As can be seen in the SEM micrograph of Figure 10(a), the adsorption of WO_4^{2-} occurs on the active sites, at which the localized attack occurred, and causes plugging of the pores. The white precipitate in the micrograph were analysed as a tungsten compound by the accompanying EDAX profile, Figure 10(b), indicating the tungstate surface layer at these sites.

Furthermore, the low inhibition influence of WO_4^{2-} compared with CrO_4^{2-}, MoO_4^{2-}, can be also attributed to the low oxidizing nature of WO_4^{2-}. WO_4^{2-} is considered as a nonoxidizing inhibitor and, hence, cannot oxidize the corrosion sites at the electrode surface.

4. Conclusions

The outcome of the present work can be summarized as follows:

(i) The pitting potential of the Al electrode moves in the positive direction by addition of CrO_4^{2-}, MoO_4^{2-} and WO_4^{2-} anions to the electrolyte, and the shift in potential increases with increase in concentration.

(ii) Chromate anions exhibit a large passivating influence during potentiostatic I/t measurements. This can be ascribed to the fact that chromate anions are a powerful oxidizing agent and capable of oxidizing the corrosion sites to give a stable Al_2O_3 film.

(iii) The inhibition observed on addition of MoO_4^{2-} anions is attributed to the adsorption and reaction of MoO_4^{2-} at the electrode forming a molybdate surface layer which selectively impedes the ingress of Cl^- ions.

(iv) XPS results confirm the presence of MoO_2, MoO_4^{2-} and MoO_3 at the electrode surface after I/t measurements and the major constituents is MoO_4^{2-} species.

(v) The adsorption of WO_4^{2-} anions at flawed areas and developing pits is the main factor for the observed inhibition, but complete passive conditions are never achieved.

References

1. M. Pourbaix, 'Atlas of Electrochemical Equilibria in Aqueous solutions' (Pergamon, 1966), p. 171.
2. P.L. Cabot, F.A. Centellas, J.A. Garrido, E. Perez and H. Vidal, *Electrochim. Acta* **36** (1991) 179.
3. S.E. Fetes, M.M. Stefenel, C. Mayer and T. Chierche, *J. Appl. Electrochem.* **20** (1990) 996.
4. H.S. Srinivasan and C.K. Mital, *Electrochim. Acta* **39** (1994) 2633.
5. Z.A. Foroulis and M.J. Thubrikar, *J. Electrochem. Soc.* **122** (1975) 1296.
6. Z.A. Foroulis and M.J. Thubrikar, *Werkst. Korros.* **26** (1975) 350.
7. S. Dallek and R.T. Foley, *J. Electrochem. Soc.* **123** (1976) 1775.
8. T.H. Nguyen and R.T. Foley, *J. Electrochem. Soc.* **127** (1980) 2563.
9. B.W. Samuels, K. Sotodudeh and R.T. Foley, *Corrosion* **27** (1981) 321.
10. P.M. Natishan, E. McCafferty and G.K. Hubler, *J. Electrochem. Soc.* **135** (1988) 321.
11. F. Hunker and H. Bohni, *Werkst. Korro.* **34** (1983) 68.
12. B.A. Shaw, G.D. Davis, T.L. Fritz and K.A. Olver, *J. Electrochem. Soc.* **137** (1990) 359.
13. M.S. Vukasovich and J.P.G. Farr, *Mater. Perform.* **25** (1986) 9.
14. M.S. Vukasovich, Corrosion 89, Paper 444, NACE, Houston, TX (1989).
15. C. Moniticelli, G. Brunoro, F. Zucchi and F. Fagioli, *Werkst. Korros.* **40** (1989) 393.
16. A. Kassab, K.M. Kamel and E. Abd El Hamid, *J. Electrochem. Soc. India* **36** (1987) 27.
17. W.A. Badawy and F.M. Al-Kharafi, *Corros. Sci.* **39** (1997) 681.
18. C.B. Breslin, G. Treacy and W.M. Carroll, *Corros. Sci.* **36** (1994) 1143.
19. A.Kh. Bairamow, S. Zakiour and C. Leygraf, *Corros. Sci.* **25** (1985) 69.
20. M.A. Stranick, Corrosion 85, Paper 380, NACE, Houston, TX (1985).
21. R.C. McCune, R.L. Shilts and S.M. Ferguson, *Corros. Sci.* **22** (1982) 1049.
22. K.M. El-Sobki, A.A. Ismail, S. Ashour, A.A. Kheder and L.A. Shalaby, *Corros. Prevent. Control* **28** (1981) 7.
23. R.R. Wiggle, V. Hospadaruk and E.A. Styloglou *Mater. Perform.* **20** (1981) 13.

24. W.C. Moshier, G.D. Davis and G.O. Cote, *J. Electrochem. Soc.* **136** (1989) 356.
25. W.C. Moshier and G.D. Davis, *Corrosion* **46** (1990) 43.
26. C.R. Clayton and Y.C. Lu, *J. Electrochem. Soc.* **133** (1986) 2465.
27. W.C. Moshier, G.D. Davis, J.S. Aheam and H.F. Hough, *J. Electrochem. Soc.* **133** (1986) 1063.
28. C.D. Wagner, W.M. Riggs, L.E. Davis, J.F. Moulder and G.E. Muilenberg (Eds) 'Handbook of X-ray Photoelectron Spectroscopy' (Perkin–Elmer Corporation, USA, 1979), p. 51.
29. T.H. Nguyen and R.T. Foley, *J. Electrochem. Soc.* **126** (1979) 1855.
30. L. Tomcsanyi, K. Varga, I. Bartik, G. Haronyi and E. Maleczki, *Electrochim. Acta* **34** (1989) 855.